

MATHEMATICAL MODELLING OF INDICATIVE PROCESS PARAMETERS OF DUAL-FUEL ENGINES WITH CONVENTIONAL FUEL INJECTION SYSTEM

Sergejus LEBEDEVAS¹, Saugirdas PUKALSKAS^{2*}, Vygintas DAUKŠYS³

^{1,3}Dept of Marine Engineering, Klaipėda University, Lithuania

²Dept of Automobile Engineering, Vilnius Gediminas Technical University, Lithuania

Received 21 June 2019; revised 25 August 2019, 22 October 2019; accepted date 21 November 2019

Abstract. Modern engine research uses multi-dimensional Mathematical Models (MMs) that are applicable to multi-fuel engines. However, their use involves the availability of detailed technical data on the design and characteristics of the engine, which is not always possible. The use of a one-dimensional MM is more expedient for the prediction of engine parameters, but their application for this purpose has not yet been sufficiently investigated. This publication presents the results of numerical studies evaluating the application of a one-dimensional MM with bi-phase Vibe combustion laws for dual-fuel (DF) Diesel (D) and Natural Gas (NG) engine power parameters. The motor test results of a high-speed 4CN79.5/95.5 Diesel Engine (DE) with a conventional fuel injection system were used as adequacy criteria. The engines were operated with D100 and DF D20/NG80, in high- (HLM), medium- (MLM), and low- (LLM) load modes, and the angle of Diesel-fuel Injection Timing (DIT) was changed from -1 to -13 °CA in the Before Top Dead Center (BTDC) range. Modelling of the single-phase Vibe combustion law has limited applicability for efficient use only in HLM (with an error of 7%). In the MLM and LLM regimes, owing to non-compliance with real bi-phasic combustion with a strongly extended NG diffusive second phase, the modelling error is 50%. Individual MM matching in MLM and LLM in a DF D20/NG80 experiment detected a burn time increase from between 45 and 50 °CA, to 110 and 200 °CA, respectively. Limited use of the one-dimensional MM in the evaluation of DF engine performance has been identified. When comparing a one-dimensional MM with experimental data, a bi-phase law of heat release characteristic should be considered for better coincidence. In addition, individual MM matching with an experiment on each engine load mode ensured acceptable accuracy in testing and optimising the parameters of the indicator process, including DIT.

Keywords: one-dimensional mathematical model, dual-fuel engine, energy indicators, heat release characteristic, single-phase combustion, bi-phase combustion.

Notations

Abbreviations:

BTDC – before top dead center [°CA];
CA – crank angle;
CC – combustion chamber;
CCR NG – co-combustion ratio of NG [%];
CFM – combustibile forest material;
D – diesel;
DE – diesel engine;
DF – dual-fuel;
DIT – D fuel injection timing [°CA];
HLM – high load mode;
HRF – high reaction fuel;
ICE – internal combustion engine;
MLM – medium load mode;

MM – mathematical model;

LLM – low load mode;

NG – natural gas.

Variables and functions:

α – excess air ratio [-];
 α_0 – nominal regime's excess air ratio [-];
 φ – current angle from the beginning of the heat release [°CA];
 φ_{cs} – start of fuel combustion [°CA];
 φ_i – induction period [°CA];
 φ_{i0} – nominal regime's induction period [°CA];
 φ_{inj} – fuel injection angle [°CA] BTDC;
 $\varphi_{P_{max}}$ – peak cycle pressure angle [°CA];
 φ_{τ_i} – induction period end [°CA];
 φ_z – conditional combustion duration [°CA];

*Corresponding author. E-mail: saugirdas.pukalskas@vgtu.lt

Φ_{z_0} – nominal regime's conditional combustion duration [°CA];
 η_e – effective efficiency coefficient [-];
 η_i – indicated efficiency coefficient [-];
 η_m – mechanical efficiency coefficient [-];
 τ – time [s];
 τ_i – induction period duration [s];
 a_1, a_2, a_3, a_4 – constants [-] (in the DE cycle, 0.8, 0.5, 0.6 and 0.5 respectively);
 c – Vibe constant;
 C, H, O – element (carbon, hydrogen, oxygen) composition in DF [%];
 C_D, H_D, O_D – element (carbon, hydrogen, oxygen) composition in D fuel [%];
 C_{NG}, H_{NG}, O_{NG} – element (carbon, hydrogen, oxygen) composition in NG [%];
 E – activation energy [J];
 f – combustion form-factor [-];
 f_0 – nominal regime's combustion form-factor [-];
 h_{ex} – exhaust gas enthalpy [J/kg];
 h_s – supply air enthalpy [J/kg];
 H_{l_D} – lower heating value of D fuel [MJ/kg];
 $H_{l_{NG}}$ – lower heating value of NG [MJ/kg];
 $H_{l_{DF}}$ – lower heating value of DF [MJ/kg];
 K_τ – constant [-];
 m_{ex} – mass of exhaust gas [kg];
 m_{inj} – mass of fuel sprayed [kg];
 m_s – supply air mass [kg];
 m_t – total mass [kg];
 n – engine speed [min^{-1}];
 n_0 – nominal regime's engine speed [min^{-1}];
 p – cycle cylinder pressure [bar];
 p_0 – ambient pressure [bar];
 p_{air} – pressure of air portion in cylinder [bar];
 p_{air_0} – nominal regime's air portion pressure in cylinder [bar];
 p_{cyl} – cylindrical pressure [bar];
 p_k – air pressure after compression [bar];
 p_{max} – maximal cylindrical pressure [bar];
 p_{me} – effective mean pressure [bar];
 p_{mi} – indicate mean pressure [bar];
 q_c – overall fuel consumption per cycle [g/cycl];
 q_{c_D} – D fuel consumption per cycle [g/cycl];
 $q_{c_{NG}}$ – NG consumption per cycle [g/cycl];
 Q – cycle heat energy [J];
 Q_{ex} – heat exchange energy [J];
 Q_f – final cycle heat release [J];
 Q_i – current cycle heat release [J];
 Q_{re} – heat release energy [J];
 R – gas constant [J/kg·K];
 R_m – molar gas constant [J/kg·K];
 T – cycle temperature [K];
 T_0 – ambient temperature [K];
 T_{air} – temperature of air portion in cylinder [K];

T_{air_0} – nominal regime's air temperature in cylinder [K];
 T_k – charged air temperature [K];
 T_t – exhaust gas temperature after turbine [K];
 U – internal energy [J];
 V – volume of cylinder [m^3];
 X – heat release ratio [-];
 X_a – abscissa anamorphosis [-];
 Y_a – ordinate anamorphosis [-].

Introduction

The use of NG for the conversion of petroleum-derived fossil fuels in DE is a promising approach for the strategic reduction of harmful emissions and greenhouse gas emissions in transport (IMO 2019a, 2019b; Arteconi *et al.* 2010; EC 2018). Numerous studies have shown that using NG in a marine DE is one of the most effective means of significantly improving the exploitation and environmental parameters of vehicles: compared to traditional marine fuels, NO_x emissions are reduced by 85...90%, CO_2 – by 10...20%, PM and SO_x are almost non-existent (Anderson *et al.* 2015; Thomson *et al.* 2015; HoC 2012; IMO 2016; Carlucci *et al.* 2009). The scientific aspects are well illustrated by the research results of the *Wartsila 20* DF single cylinder marine engine (García Valladolid *et al.* 2017). In the context of the *Tier III* level limitation, the authors investigated the principles of rational control of the engine indicator working process necessary to achieve a usually high environmental level without the use of expensive exhaust gas purification technologies. Comprehensive experimental and numerical studies have justified the optimal value of the space and time distribution of a rational pilot portion of liquid fuel injected into the CC as a method of controlling the DF combustion process. As a result, the NO_x concentration in the exhaust gas is reduced from 3000 to 500 mg/Nm^3 , which is below the *Tier III* level in a wide engine operating range ($p_{me} = 2.1...1.3$ bar). In parallel with extensive experimental studies (García Valladolid *et al.* 2017; Papagiannakis *et al.* 2010; Yousefi *et al.* 2015; Mustafi *et al.* 2013), at least as much attention is being paid to the development of mathematical modelling technology research (Maurya, Mishra 2017; Abagnale *et al.* 2014). Multi-dimensional MM are preferred among numerical models. When implemented in software packages, multi-dimensional MMs are effective at solving systems of moment (Navje–Stokes), energy (Furje–Kirghof), and mass-endurance equations – e.g., FIRE (AVL, Austria), KIVA (Laboratory of Energy Research, US), and VECTIS (Ricardo, England). Versatile software platforms such as FLUENT, ANSYS/Flotran, Star CD, and PHOENIX are also commonly used to solve individual numerical and reciprocating type ICE design challenges (Kakaee *et al.* 2015; Liu *et al.* 2015; Rapalis *et al.* 2013). Based on MM benchmarking sources (Kavtaradze 2008), one of the most common is the CFM MM (Heider 1996; Heider *et al.* 1998), which is applied to cases in which gas is premixed before delivery to the cylinder. In the case of mixed gases

under high-temperature and pressure conditions, refined equations by Metghalchi and Kech are used (Janbozorgi *et al.* 2009). In the work by Merker *et al.* (2006) on DE conversion problems, extended CFM has all the features of the standard CFM model and the modernized CFM upgrade. The model has been expanded mainly for modelling combustion in petrol engines with direct fuel spraying. For example, in FIRE, it is used to implement the SPRAY software application to simulate the fuel injection process. The CFM model, as well as its various modifications, has been well tested to investigate the performance of DF engines. These models have been converted to calculate the combustion process of gaseous fuel in both ICE with spark ignition and DF engines with gas fuel ignition from a pilot portion of D fuel. To study the formation of toxic components, particularly NO_x, the model developed by Heider (Heider *et al.* 1998; Liu *et al.* 2015) is widely used.

One of the main advantages of using multi-dimensional MMs in practice is the wide range of possibilities for thoroughly investigating the physical processes of rapid engine transformation and the formation of harmful components in the engine cylinder. The optimization of these physical processes provides the basis for improving the energy efficiency and ecological parameters of NG-powered engines (García Valladolid *et al.* 2017; Nithyanandan *et al.* 2016; Hosmath *et al.* 2016; Li *et al.* 2016; Wang *et al.* 2017). For example, García Valladolid *et al.* (2017), mathematical modelling techniques in DF engines have been used to investigate the dynamics of the physical interaction between the gaseous and fuel liquid phases – the influence of the pilot fuel distribution structure in the cylinder on the NG combustion process. It is reasonable to assume that the angle of the pilot fuel injection rate determines the reaction properties of the combustible mixture, which is evaluated by the distribution coefficient of the air utilization factor, as well as the influence of the CC thermodynamic parameters. In research by Maurya and Mishra (2017), the combustion and ecological characteristics of a 6-cylinder 130/112 engine with a 3D CFD MM DF analysis were investigated using STAR-CD software. The relationships among engine operating parameters, temperature, and harmful component fields in the CC were identified and investigated (García Valladolid *et al.* 2017). The CFD dynamic model used for this study is implemented in the AVL FIRE-CHEMICIN software. The activity field of the active radical distribution of OH radicals in the work mixture, at the previous angle of the pilot fuel injection, provides an energy efficiency improvement of 7.5% and a five- to six-fold reduction in harmful emissions of C_nH_m, CO and NO_x. Therefore, in the initial research phase in addition to the modern practice of multi-dimensional ICE MMs, including conversions to DF engines, well-approved one-dimensional and phenomenological MMs agree with the results of experimental research (Ivanchenko *et al.* 1983; Lebedev *et al.* 2003). This result is typical of the preliminary performance of existing DEs fleet models, showing the efficiency of the transfer to NG in the absence of initial data for the effi-

cient use of multi-dimensional models. In addition, mathematical modelling of the closed balance of a piston and a turbocharged engine is important for solving technical problems in converting existing engines to DF (D/NG) and for evaluating engine performance. In practice, these modelling capabilities in DE research are well characterized by one-dimensional MMs, but their effective use in convertible DEs requires an assessment of their conditions of use, which has not yet been thoroughly studied.

Analogous work has been performed by researchers at Klaipėda University and Vilnius Gediminas Technical University on a high-speed 4C_{79.5/95.5} Diesel Engine (DE) retrofitted to function on a DF D/NG cycle to assess energy efficiency and ecological sustainability. The purpose of the research presented in this publication was to evaluate the efficiency of a one-dimensional MM in the IMPULS software program, to determine the energy and ecological indicators of a conventional fuel injection system during different engine operating modes. The influence of the change in the injection phase of the pilot fuel portion was also assessed. The results of mathematical modelling are compared with experimental engine test result data.

1. Methodological basics

For the numerical research transfer function, a one-dimensional MM (Ivanchenko *et al.* 1983) with a formalised heat transfer law in Vibe was used to calculate the characteristics and energy parameters of the NG DE (Merker *et al.* 2006).

1.1. Mathematical model

The studies used a one-dimensional MM implemented in the IMPULS software (Ivanchenko *et al.* 1983). The software simulates a closed DE model, both with and without an inflated work process. This is based on quasi-static equations of thermodynamics and gas dynamics, considering the parameters of the exhaust system design, variable gas turbine and compressor efficiency coefficients, heat losses to the engine cooling system, and ambient air parameters. The processes in the engine cylinder are described by a system of differential equations consisting of the laws of energy, the mass and state – Equations (1)–(3):

$$\frac{dU}{d\tau} = \frac{dQ_{re}}{d\tau} - \frac{dQ_{ex}}{d\tau} - p \cdot \frac{dV}{d\tau} + h_s \cdot \frac{dm_s}{d\tau} - h_{ex} \cdot \frac{dm_{ex}}{d\tau} \quad [\text{kJ/s}]; \quad (1)$$

$$\frac{dm_t}{d\tau} = \frac{dm_s}{d\tau} + \frac{dm_{inj}}{d\tau} - \frac{dm_{ex}}{d\tau} \quad [\text{kg/s}]; \quad (2)$$

$$\frac{dp}{d\tau} = \frac{m_t \cdot R}{V} \cdot \frac{dT}{d\tau} + \frac{m_t \cdot T}{V} \cdot \frac{dR}{d\tau} + \frac{R \cdot T}{V} \cdot \frac{dm_t}{d\tau} - \frac{p}{V} \cdot \frac{dV}{d\tau} \quad [\text{Pa/s}]. \quad (3)$$

Heat isolation is realized by the Vibe model (Equation (4)) with additions by Woschni Equations (5) and (6), which are widely used to study ICE work process modelling (Merker *et al.* 2006):

$$X = 1 - e^{-6.908 \left(\frac{\varphi}{\varphi_z} \right)^{f+1}} \quad [-]; \quad (4)$$

$$f = f_0 \cdot \left(\frac{\varphi_{i_0}}{\varphi_i} \right)^{a_2} \cdot \left(\frac{p_{air_0}}{p_{air}} \right) \cdot \left(\frac{T_{air_0}}{T_{air}} \right) \cdot \left(\frac{n_0}{n} \right)^{a_1} \quad [-]; \quad (5)$$

$$\varphi_z = \varphi_{z_0} \cdot \left(\frac{\alpha_0}{\alpha} \right)^{a_3} \cdot \left(\frac{n_0}{n} \right)^{a_4} \quad [^\circ\text{CA}]. \quad (6)$$

An important induction cycle induction period for indicator cycle modelling is determined by the compression iterative method – Equations (8)–(10):

$$\varphi_i = 6 \cdot n \cdot \tau_i \quad [^\circ\text{CA}]; \quad (8)$$

$$\tau_i = K_\tau \cdot 10^{-5} \cdot \left(\frac{T}{p} \right)^{0.5} \cdot \exp\left(\frac{E}{R_m \cdot T} \right) \quad [\text{s}]; \quad (9)$$

$$\frac{1}{6 \cdot n} \cdot \int_0^{\varphi_i} \frac{d\varphi}{\tau_i} = 1 \quad [-]. \quad (10)$$

The MM was supplemented and modified to model a DF engine: an additional software block was programmed, which calculates the energy mix of the work mixture (specific heat, enthalpy, internal energy, lower calorific value) according to the actual elemental composition of the DF.

For the calculation of the initial program data, the cyclic portion q_c of the dual D-NG fuel with chemical elemental composition (C, H, O) is determined as follows.

Fuel consumption per cycle evaluated by Equation (11):

$$q_c = \frac{q_{c_D} \cdot H_{l_D} + q_{c_{NG}} \cdot H_{l_{NG}}}{H_{l_{DF}}} \quad [\text{g/cycl}]. \quad (11)$$

The lower heat value of the fuel is calculated by the Mendeleev Equation (12):

$$H_{l_{DF}} = 337.5 \cdot C + 1025 \cdot H - 108.3 \cdot O \quad [\text{MJ/kg}], \quad (12)$$

where:

$$C = C_D \cdot (100 - \text{CCR NG}) + C_{NG} \cdot \text{CCR NG};$$

$$H = H_D \cdot (100 - \text{CCR NG}) + H_{NG} \cdot \text{CCR NG};$$

$$O = O_D \cdot (100 - \text{CCR NG}) + O_{NG} \cdot \text{CCR NG}.$$

Table 1. Engine specifications

Model	4ČN79.5/95.5
Displacement [cm ³]	1896
Bore × stroke [mm]	79.5 × 95.5
Maximum power [kW] / [rpm]	66 / 4000
Maximum torque [N · m] / [rpm]	180 / 2000...2500
Cooling type	Water cooling
Fuel supply system	Electronic controlled Bosch VP37 distribution type fuel pump, one phase direct injection
No of cylinders	4 in line
Compression ratio	19.5:1
Aspiration	Turbocharge

Co-combustion ratio of natural gas evaluated by Equation (13):

$$\text{CCR NG} = \frac{q_{c_{NG}} \cdot H_{l_{NG}}}{q_{c_{NG}} \cdot H_{l_{NG}} + q_{c_D} \cdot H_{l_D}} \cdot 100\%. \quad (13)$$

1.2. Test engine and fuel specification

The object of the research was a high-speed 4ČN79.5/95.5 DE with a conventional “boot type” fuel injection system (Breitbach 2002; Bosch 2002). The DE main specific parameters are listed in Table 1.

Alignment of the MM with the subject of the study, as well as the evaluation of the modelling results, was performed in comparison with the experimental results carried out on the engine operating on DF. During DF mode engine construction, its system parameters remained unchanged, except for the fuel injection angle φ_{inj} , which was changed in the range from -1 to -13 °CA BTDC.

The test bench and test equipment are described in detail in the researches by Rimkus *et al.* (2016, 2017).

Two types of fuel were used during the experiment – D and NG. The D fuel was under the EN 590:2013+A1:2017 standard and the compressed NG was under the ISO 6976:2016 standard (Table 2).

Table 2. Fuel properties

	Fuel type		
	NG	D	EN 590:2013+A1:2017
Density [kg/m ³]	0.74	832.0	820...845
Cetane number	–	51.3	51...52.2
Lower heat value [MJ/kg]	51.7	42.8	–
Viscosity [cSt 40a°C]	–	2.72	2...4.5
H/C ratio	–	1.907	–
Component [% vol.]	Methane: 91.97 Ethane: 5.75 Propane: 1.30 Butane: 0.281 Nitrogen: 0.562 Carbon dioxide: 0.0	Carbon: 86.0 Hydrogen: 13.6 Oxygen: 0.4	–

1.3. Engine test modes

Experimental data were used to evaluate MM simulation results on a wide range of engine operating modes (Lebedevas *et al.* 2019). In each operating mode, characterized by the combination $-p_{me}, n, \varphi_{inj}$, the engine parameters were investigated using pure D, DF D/NG according to the compositions D60/NG40, D40/NG60, and D20/NG80 (where the figures for the D and NG indices correspond to the percentages of D and NG expressed as a percentage of the total fuel energy balance). When the engine is running at $p_{me} = 5.97$ bar, the mode is called HLM; at $p_{me} = 3.99$ bar, the mode is called MLM; at $p_{me} = 1.98$ bar, the mode is called LLM. The obtained experimental results showed a consistent deterioration in energy parameters due to an increase in the share of NG in the fuel composition. Therefore, to compare the results of mathematical modelling and experimental studies, only two options were investigated: an engine running on pure D fuel and on a fuel mixture D20/NG80, i.e. with the maximum proportion of NG used in the studies.

The compatibility of MM with the research object was tested according to the engine's HLM parameters for D. When modelling the engine parameters in partial load modes with DF D-NG, as well as φ_{inj} variations, the parameters of the engine's matching MM were not changed.

The mathematical simulation results were evaluated by comparing them with experimental data obtained by averaging 5 tests at steady state.

2. Research results and discussion

In the initial stage of the research, the MM was coordinated with the object under investigation in HLM D ($\varphi_{inj} = -13^\circ\text{CA BTDC}$). The constants used in the MM algorithm, including the Woschni Equations (5), (6) and the turbo aggregate characteristics, were left unchanged while performing engine parameter simulation in partial-load MLM and LLM modes; only φ_{inj} was changed in the range from -1 to -13°CA BTDC . The results are compared to the experimental data in Table 3.

One-dimensional MMs, designed primarily for modelling and optimizing the effective energy parameters of an engine $-p_{me}, T_p, p_{max}, p_k, T_k$, and are poorly used to modelling real physical processes in a cylinder (Ivanchenko *et al.* 1983; Merker *et al.* 2006). The applicability of these MMs to the study of indicative process characteristics is generally limited, mainly due to the actual formalization of combustion and heat exchange processes. The results of the research confirm the good correspondence of the simulation results of the effective parameters and the indicator diagrams (determining p_{me}) with the experimental data (Table 3 and Figure 1). For the reasons mentioned above, the current cycle parameters of the indicator process $-T, Q = f(\varphi)$, have increased errors up to 15...18%. The error of mathematical modelling of the engine effective energy parameters in HLM and MLM load modes does not exceed 40...5%, in LLM mode 7...15%.

Table 3. Comparison of the high-speed 4CŃ79.5/95.5 DE parameters functioning in the D fuel experiment and MM parameters $n = 2000 \text{ min}^{-1}$

	Fuel: D					
	$p_{me} = 5.97 \text{ bar}$		$p_{me} = 3.99 \text{ bar}$		$p_{me} = 1.98 \text{ bar}$	
	-1	-13	-1	-13	-1	-13
$\varphi_{inj} [^\circ\text{CA}] \text{ BTDC}$	-1	-13	-1	-13	-1	-13
$p_k [\text{bar}]$	1.52/1.53	1.42/1.42	1.36/1.36	1.267/1.27	1.19/1.21/1.22*	1.17/1.17/1.17*
$\alpha [-]$	2.87/2.58	2.92/2.55	3.76/3.27	3.59/3.14	5.38/4.81/4.56*	5.22/4.62/4.36*
$T_t [\text{K}]$	703/719	659/646	621/619	594/579	535/515/525*	524/490/582*
$T_k [\text{K}]$	338/345	333/332	326/326	323/322	316/310	319/318/318*
$p_0 [\text{bar}]$	1.0	1.0	1.0	1.0	1.0	1.0
$T_0 [\text{K}]$	278	277	275	281	278	281
$q_c [\text{g/cycl}]$	0.01949	0.01826	0.01407	0.01364	0.00897/0.0095*	0.00876/0.0093*
$p_{max} [\text{bar}]$	69.4/66.4	105.8/105.4	59.1/57.4	92.0/94.0	52.2/50.0/52*	80.3/83.6/83.7*
$\varphi_{cs} [^\circ\text{CA}]$	8/8.6	-6/-6	7/7	-5/-5	11/9/9*	-4/-4/-4*
$\varphi_{p_{max}} [^\circ\text{CA}]$	11/10	5/6	10/9	5/5	13/12/12*	2/2/2*
$p_{me} [\text{bar}]$	5.96/5.67	5.96/5.80	3.98/3.85	3.98/3.85	1.99/1.75/1.98*	1.99/1.70/1.95*
$p_{mi} [\text{bar}]$	8.20/7.80	8.20/7.95	6.24/6.00	6.24/6.00	4.42/3.90/4.15*	4.42/3.86/4.1*
$\eta_m [-]$	0.73/0.73	0.73/0.73	0.635/0.64	0.635/0.64	0.45/0.45/0.45*	0.45/0.44/0.45*
$\eta_e [-]$	0.339/0.330	0.362/0.352	0.313/0.304	0.323/0.313	0.245/0.216/0.23*	0.251/0.215/0.23*
$\eta_i [-]$	0.477/0.456	0.509/0.483	0.493/0.472	0.492/0.488	0.545/0.482/0.425*	0.559/0.488/0.49*

Notes:

- in the experiment and MM results, q_c was increased by 5% to approximate the cylinder load unevenness;
- in table, for example, values 1.19/1.21/1.22* means, first value is from experiment, second is from MM and third is MM with q_c increased by 5%.

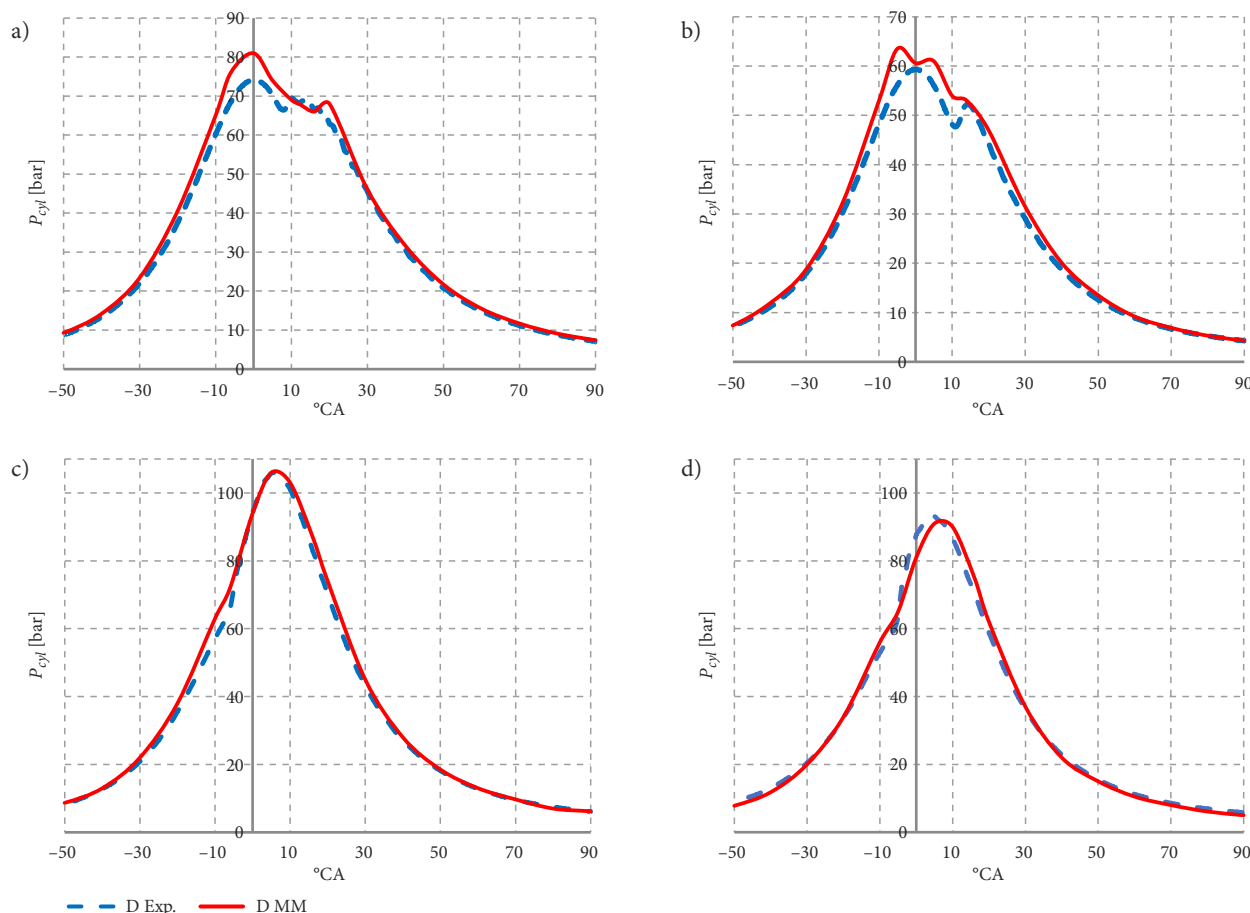


Figure 1. Comparison of the experiment and mathematical modelling indicator diagram parameters of the 4C7N79.5/95.5 engine functioning on D fuel: a – D100, $p_{me} = 5.97$ bar, $\varphi_{inj} = -1^\circ\text{CA}$ BTDC; b – D100, $p_{me} = 1.98$ bar, $\varphi_{inj} = -1^\circ\text{CA}$ BTDC; c – D100, $p_{me} = 5.97$ bar, $\varphi_{inj} = -13^\circ\text{CA}$ BTDC; d – D100, $p_{me} = 3.99$ bar, $\varphi_{inj} = -13^\circ\text{CA}$ BTDC

The MM of the IMPULS software works as follows: f and φ_z are set to one mode (mainly peak power), and in intermediate load modes they are recalculated according to Woschni's statistically determined analytical dependencies – φ_i , p_0 , T_0 , α , n (Merker *et al.* 2006). The good correlation between the mathematical modelling results and the experimental engine parameters indicates the arrangement of the MM with the engine running on diesel, once again confirming the functionality of the Woschni model. At the next stage of research, the effectiveness of applying a MM to calculate the change in engine parameters for working on a D20/NG80 fuel mixture ($p_{me} = 1.98 \dots 5.97$ bar) was evaluated. This confirms the appropriateness of using an MM for D-NG engine modelling at HLM, MLM, and LLM load modes at $\varphi_{inj} = -1 \dots -13^\circ\text{CA}$ BTDC, CCR NG 0.8 (or an engine running on D20/NG80 fuel). The modelling results are presented in Table 4. The results are positively evaluated by simulation in HLM only. The difference between the experimental and modelling parameters does not exceed 2...6% (Table 5).

In partial load modes, the MLM and LLM modelling error is up to 50% (Table 6). Notably, the most important discrepancy in the energy parameters – p_{me} , p_{mi} , η_e , η_i is in range of 15...52%.

The large difference in the modelled indicators was obtained under practically uniform conditions of work process execution and modelling: φ_{cs} , p_k , T_k , φ_i and q_c . On this basis, it is hypothesised that the deviations of the modelling results for the small regimes of p_k in the difference with the experiment are associated with the loss of the gaseous fuel during the purge phase. In HLM ($p_{me} = 5.97$ bar), the amount of gaseous fuel lost is not high, but its size in LLM $p_{me} = 1.98$ bar is increasing. On the other hand, deviations of η_e and η_i are associated with a significant impact on the increase in DF burning time.

The first suspicion has not been confirmed in the assessment of harmful component emission. The conversion of CH_4 from the gaseous fuel into the HC emissions does not exceed -42 g/h in MLM and -60 g/h in LLM (or 1.3 and 2.2%, respectively) of used NG DF D20/NG80. On the other hand, a significant increase in the duration of the heat release characteristic in the functioning of the D20/NG80 was confirmed by the experimental data. For example, 50% of the heat release in the HLM increases by only 4°CA , whereas in MLM and LLM, it increased by 12°CA and 42°CA , respectively. The results of the engine indicator process simulation also confirm the observed peculiarity.

Table 4. Comparison of the experimental and MM parameters of the high-speed 4ĈN79.5/95.5 DE in DF D/NG mode, $n = 2000 \text{ min}^{-1}$

	DF: D20/NG80			
	$p_{me} = 5.97 \text{ bar}$		$p_{me} = 3.99 \text{ bar}$	$p_{me} = 1.98 \text{ bar}$
$\phi_{inj} [\text{°CA}] \text{ BTDC}$	-1	-13	-1	-1
$p_k [\text{bar}]$	1.47/1.45	1.35/1.34	2.38/1.36	1.25/1.28
$\alpha [-]$	2.30*/2.28**	2.54*/2.23**	2.57*/2.54**	2.93*/3.0**
$T_t [\text{K}]$	750/783	661/690	661/793	571/720
$p_k [\text{bar}]$	343/342	333/335	329/336	319/325
$q_c [\text{g/cycl}]$	0.01975/	0.01695	0.01746	0.01457
$p_{max} [\text{bar}]$	64.2/62.8	99.7/99.5	57.8/74.1	50.1/70.5
$\phi_{cs} [\text{°CA}]$	7/7	-5/-5	8/9.5	11/11
$p_{me} [\text{bar}]$	5.964/6.00	5.964/6.08	3.976/5.18	1.988/4.1
$p_{mi} [\text{bar}]$	8.204/8.14	8.204/8.25	6.242/7.32	4.194/6.25
$\eta_m [-]$	0.727/0.73	0.727/0.73	0.637/0.71	0.474/0.65
$\eta_e [-]$	0.288/0.310	0.366/0.348	0.218/0.293	0.131/0.27
$\eta_i [-]$	0.396/0.42017	0.462/0.473	0.342/0.415	0.275/0.424

Note: */** – experiment excess air ratio / MM excess air ratio.

Table 5. Comparison of the experimental and MM parameters of the high-speed 4ĈN79.5/95.5 DE operating in D20/NG80 HLM $p_{me} = 5.97 \text{ bar}$, $n = 2000 \text{ min}^{-1}$

	$p_k [\text{bar}]$	$\alpha [-]$	$T_t [\text{K}]$	$T_k [\text{K}]$	$p_{me} [\text{bar}]$	$p_{mi} [\text{bar}]$	$\eta_e [-]$	$\eta_i [-]$
$\phi_{inj} = -13 \text{ °CA BTDC}$	1.35/1.35	2.54/2.67	661/686	333/324	5.964/5.71	8.204/7.82	0.366/0.333	0.462/0.456
Error [%]	0	+5.1	+3.6	-2.8	-4.5	-4.9	-10.0	-1.3
$\phi_{inj} = -1 \text{ °CA BTDC}$	1.47/1.44	2.30/2.41	750/808	343/342	5.964/6.00	8.204/8.14	0.288/0.310	0.396/0.417
Error [%]	-2.1	+4.78	+7.18	-0.3	+0.6	-0.8	+7.1	5.0

Table 6. Comparison of the experimental and MM parameters of the high-speed 4ĈN79.5/95.5 DE operating in D20/NG80 in partial load modes MLM and LLM, $n = 2000 \text{ min}^{-1}$

	$p_k [\text{bar}]$	$\alpha [-]$	$T_t [\text{K}]$	$T_k [\text{K}]$	$p_{max} [\text{bar}]$	$p_{me} [\text{bar}]$	$p_{mi} [\text{bar}]$	$\eta_e [-]$	$\eta_i [-]$
$p_{me} = 3.99 \text{ bar}$	1.38/1.36	2.57/2.54	661/793	329/336	57.8/74.1	3.976/5.18	6.242/7.32	0.218/0.293	0.342/0.415
Error [%]	-1.5%	-1.2%	+16.6	+2.1	+22.0	+23.0	+14.7	+25.6	+17.6
$p_{me} = 1.98 \text{ bar}$	1.25/1.28	2.93/3.0	571/720	319/325	50.1/70.5	1.988/4.1	4.194/6.25	0.131/0.27	0.275/0.424
Error [%]	+2.3	+2.4	+20.7	+1.8	+29.0	+51.5	+32.9	+51.5	+35.1

Mathematical modelling was accomplished by a variation of the method developed by Bulaty and Glanzmann (1984). For each operation mode, the actual values of f and ϕ_z are given in Table 7.

Unlike engine performance with D fuel, the load drop ϕ_z from 65 °CA in HLM increased to 110 °CA and 200 °CA in MLM and LLM, respectively, although the excess air factor α increased from 2.3 to 2.5 and 2.93, respectively. According to Equation (6), ϕ_z should instead decrease to 61 °CA and 56 °CA, respectively. When the engine ran on D fuel, ϕ_z decreased with increasing energy efficiency parameters, especially η_p , as α did in the partial-load modes.

An obvious discrepancy between the ϕ_z values was obtained based on the experiment and analytical expression – Equation (4). Therefore, the analytical ϕ_z determination method for dual engine fuelling must be rationalised.

The physical cause of this fact, as determined by the results of experimental studies (Zhang *et al.* 2017; Yousefi *et al.* 2017), reveals peculiarities of the DF combustion process structure and phase change compared to the indicator D process. After the kinetic HRF phase, the next phase of combustion is the combustion of gaseous fuel from the kinetic and diffusive mechanism. The intensity of NG combustion depends on the spread of active radicals in the cylinder. In the absence of sufficient time to prepare for the NG diffusion phase, the insufficient HRF induction period length NG burning process extends with all visible η_i effects.

Table 8 shows the parameters of the 4ĈN 79.5/95.5 engine when operating on the DF D20/NG80 mode, along with the modelling results, using the corrected f and ϕ_z correlation dependence on the parameters α , p_k , T_k and n .

Table 7. High-speed 4ĈN79.5/95.5 DE Vibe heat release law model parameters, $n = 2000 \text{ min}^{-1}$

	$p_{me} = 5.97 \text{ bar}$		$p_{me} = 3.99 \text{ bar}$		$p_{me} = 1.98 \text{ bar}$	
	$p_{mi} = 8.2 \text{ bar}$		$p_{mi} = 6.2 \text{ bar}$		$p_{mi} = 4.4 \text{ bar}$	
	D	D20/NG80	D	D20/NG80	D	D20/NG80
$f [-]$	0.8	0.6	0.7	0.6	0.64	0.6
$\varphi_z [^\circ\text{CA}]$	50	65	44	110	35	200
$p_k [\text{bar}]$	1.421	1.35	1.27	1.25	1.17	1.18
$T_k [\text{K}]$	333	333	323	318	319	318
$\varphi_i [^\circ\text{CA}]$	7	8	8	9	9	10
$\alpha [-]$	2.92/2.55*	2.54/2.23*	3.59/3.14*	2.95/2.49*	5.22/4.62*	3.19/2.71*

Note: * – experiment excess air ratio / MM excess air ratio.

Table 8. Mathematical modelling of the high-speed 4ĈN79.5/95.5 DE functioning DF D20/NG80 mode indicators using revised f and φ_z parameters ($\varphi_{inj} = -13 \text{ }^\circ\text{CA BTDC}$)

	$p_{me} = 5.97 \text{ bar}$		$p_{me} = 3.99 \text{ bar}$		$p_{me} = 1.98 \text{ bar}$	
	Exp.	MM	Exp.	MM	Exp.	MM
$q_c [\text{g/cycl}]$	0.0169	0.0169	0.0143	0.0143	0.01255	0.01255
$H_{iDF} [\text{MJ/kg}]$	48.33	48.33	48.48	48.48	48.55	48.55
$p_k [\text{bar}]$	1.35	1.35	1.25	1.25	1.175	1.175
$T_k [\text{K}]$	333	333	318	318	315	315
$p_{max} [\text{bar}]$	100.6	100.0	79.0	76	67.3	66.3
$\eta_e [-]$	0.345	0.345	0.273	0.276	0.155	0.157
$\eta_i [-]$	0.475	0.473	0.433	0.438	0.330	0.333
$\eta_m [-]$	0.726	0.730	0.630	0.630	0.470	0.470
$p_{me} [\text{bar}]$	5.95	5.96	3.97	4.05	1.98	2.00
$p_{mi} [\text{bar}]$	8.20	8.17	6.30	6.40	4.20*	4.28
$\alpha [-]$	2.54	2.23	2.95	2.49	3.19	2.71

With the exception of the exhaust gas temperature T_p , the energy parameters of the DF engine MM (p_{max} , η_i , η_e , p_{mi} , p_{me}) with a sufficient accuracy of 3...5% correspond to the experimental data. The T_t mismatch is explained by the simulation of the bi-phase real combustion process in one-dimensional heat release characteristics – Equation (4). Kinetic D and NG combustion phases forming p_{max} , as well as η_i and p_{mi} are well described by f and φ_z . The further phase of NG diffusion, prolonged combustion, determines the value of T_t . However, the single-phase heat release model is incomplete, as evidenced by modelling. This indicates that a single-phase Vibe combustion model for DF engines does not correspond to the adequacy of the T_t parameter setting and must be modified to a bi-phase combustion model (Maurya, Mishra 2017; Abagnale et al. 2014; Maghbouli et al. 2013). To confirm this (Figure 2), which shows the experimental heat release characteristics of the engine under the D and DF D20/NG80 fuel logarithmic anamorphosis (Merker et al. 2006).

D fuel performance is accurately approximated by a single linear segment, which means a single-phase form. With DF D20/NG80 fuel, two distinct linear segments with different angular coefficients indicate two stages of the combustion process. One of the measures to improve the energy performance of DF engines is to optimise the DIT.

Experimental studies by García Valladolid et al. (2017), Wang et al. (2017), Zhang et al. (2017) and Yousefi et al. (2017) highlight improvements of dual-engine energy and ecological parameters optimised for DIT – up to $-50 \text{ }^\circ\text{CA BTDC}$. Thus, using a one-dimensional model for changing the DIT is appropriate for an engine functioning on both D and DF. Data on an engine functioning with D fuel are presented in Table 3, and data on DF D20/NG80 fuel with a range of DIT change from -1 to $-13 \text{ }^\circ\text{CA BTDC}$ are given in Table 9.

The differences in modelling and experimental data has error from 5 to 7% in the use of a one-dimensional MM for optimising convertible DF engines with a conventional fuel injection system's DIT optimisation.

Thus, a precondition for the effective use of a one-dimensional MM is its agreement with experimental data for each mode of the simulated load. It is also rational to use a two-phase heat release model instead of a single-phase. The mathematical modelling techniques of one-dimensional models can reasonably be combined with statistical experimental data. Figure 3 (three lines) shows an example of correlative graphical dependencies provided by $\eta_i = f(\alpha, p_{me} - \text{idem})$ according to the author's experimental data. Estimating three different load regimes p_{me} is kept idem.

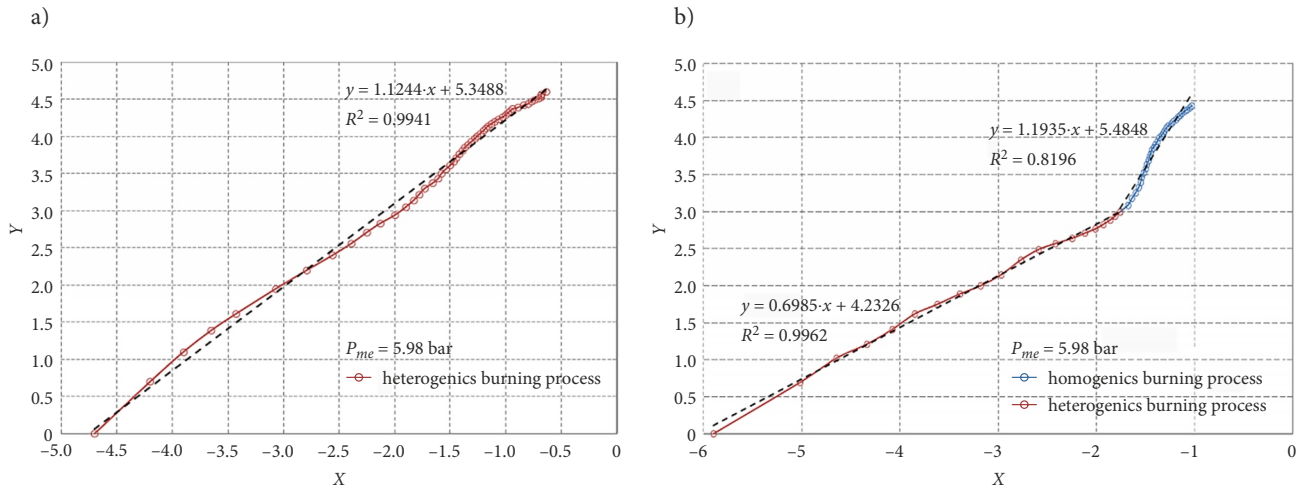


Figure 2. Logarithmic anamorphosis of high-speed 4ĊN79.5/95.5 DE functioning with D and DF D20/NG80 fuel heat extraction

characteristics: $X_a = -\ln\left(\ln\left(1 - \frac{Q_i}{Q_f}\right) + \ln(c)\right)$, $Y_a = \left(\frac{1}{f+1}\right) \cdot X + \ln(\varphi_z)$, $c = -6.908$: a – D fuel; b – DF D20/NG80 fuel

Table 9. High-speed 4ĊN79.5/95.5 DE functioning on DF D20/NG80 fuel mode with DIT range from –1 to –13 °CA BTDC mathematical modelling results

	$p_{me} = 5.97$ bar		$p_{me} = 3.99$ bar		$p_{me} = 1.98$ bar	
	Exp.	MM	Exp.	MM	Exp.	MM
p_k [bar]	1.47	1.45	1.38	1.37	1.25	1.26
α [-]	1.84	2.28	2.05	2.55	2.3	2.83
T_k [K]	343	342	333	336	323	323
q_c [g/cycl]	0.01975	0.01975	0.01746	0.01746	0.01457	0.0150
φ_{cs} [°CA]	7	7	8	9	11	11
p_{me} [bar]	5.96	6.00	4.00	4.30	2.00	1.87
p_{mi} [bar]	8.20	8.12	6.24	6.6	4.20	4.00
η_m [-]	0.730	0.730	0.640	0.640	0.470	0.430
η_e [-]	0.288	0.310	0.218	0.240	0.131	0.121
η_i [-]	0.396	0.417	0.342	0.370	0.275	0.257
p_{max} [bar]	64.2	62.8	57.8	55.0	50.1	48.4

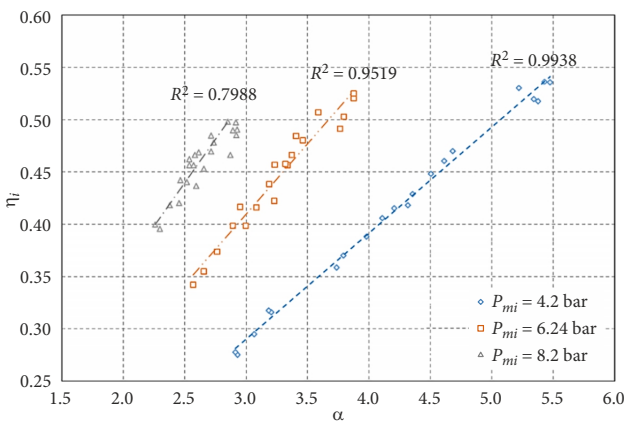


Figure 3. DF engine η_i and α parameter relation during different loads CCR NG and φ_{inj} (CCR NG = 0...0.8; $\varphi_{inj} = -1...-13$ °CA BTDC)

To determine the energy efficiency indicators η_i of an engine under both a D load and a DF D/NG load (p_{me} – idem) in a given load mode, it is sufficient to evaluate α . The rational DIT phase is chosen to be modelled by customising the MM to each engine load mode with experimental data. The research results show limited possibilities for simulating a one-dimensional MM with formalised heat release characteristics for simulating the DF engine indicator processes. For a deeper understanding of DF engine indicator processes and the heat release mechanism in the engine cylinder, the authors continue the research on that topic by using multi-dimensional mathematical modelling software AVL FIRE. The authors are very thankful to AVL List GmbH for providing the AVL FIRE software.

Conclusions

Numerical studies using multi-dimensional MM have become one of the most important components in the development of DE conversion to DF (D/NG) technology. At the same time, in the initial stages of research and in solving technological problems of engine design modification, in parallel with multi-dimensional MM rational one-dimensional MM, which implement closed energy balance of piston engine part and air inflator, are applied.

The aim of the research carried out by the authors was to supplement the information lacking in the literature on the possibilities of rational use of a one-dimensional MM for the investigation of the parameters of the DF engine indicated process; the subject of the research was a high-speed 4ČN79.5/95.5 DE with a traditional fuel injection system.

A one-dimensional MM with a formalized single-phase heat release characteristic has limited applications. One of the main reasons for this is the intense lengthening of the fuel combustion process with dual fuel in medium ($p_{me} = 3.99$ bar) and low ($p_{me} = 1.98$ bar) load modes: compared to high ($p_{me} = 5.97$ bar) load modes the difference is 1.7 and 3 times respectively. The use of one-dimensional MM in the mathematical modelling of DF engines is rational for the prediction of the effective energy parameters of the engine (p_{me} , η_e , p_k , T_k etc.), since the modelling errors of the indicated process parameters reach up to 15%. It is also necessary to reconcile the one-dimensional MM with the experimental data for each simulated engine partial load mode.

In the next stage of research, it is planned to evaluate the adequacy of one-dimensional MM functionality by changing the single-phase heat characteristic to bi-phase, in order to expand the utilization of single-zone MM for modelling the parameters of the motor indicated process.

Acknowledgements

The authors are grateful to AVL Advanced Simulation Technologies for providing the AVL FIRE simulation software.

AVL FIRE was acquired by signing a cooperation agreement between AVL Advanced Simulation Technologies and the Faculty of Marine Technologies and Natural Sciences of Klaipėda University.

References

- Abagnale, C.; Cameretti, M. C.; De Simio, L.; Gambino, M.; Iannaccone, S.; Tuccillo, R. 2014. Numerical simulation and experimental test of dual fuel operated diesel engines, *Applied Thermal Engineering* 65(1–2): 403–417. <https://doi.org/10.1016/j.applthermaleng.2014.01.040>
- Anderson, M.; Salo, K.; Fridell, E. 2015. Particle- and gaseous emissions from an LNG powered ship, *Environmental Science & Technology* 49(20): 12568–12575. <https://doi.org/10.1021/acs.est.5b02678>
- Arteconi, A.; Brandoni, C.; Evangelista, D.; Polonara, F. 2010. Life-cycle greenhouse gas analysis of LNG as a heavy vehicle fuel in Europe, *Applied Energy* 87(6): 2005–2013. <https://doi.org/10.1016/j.apenergy.2009.11.012>
- Bosch, R. 2002. *Dieselmotor-Management*. Vieweg+Teubner Verlag, Wiesbaden GmbH. 479 S. <https://doi.org/10.1007/978-3-322-99413-4> (in German).
- Breitbach, H. 2002. *Fuel Injection Systems Overview*. Delphi Corporation, Gillingham, UK.
- Bulaty, T.; Glanzmann, W. 1984. Bestimmung der Wiebe-Verbrennungsparameter, *MTZ – Motortechnische Zeitschrift* 45(7–8): 299–303. (in German).
- Carlucci, A. P.; Laforgia, D.; Saracino, R. 2009. Effects of in-cylinder bulk flow and methane supply strategies on charge stratification, combustion and emissions of a dual-fuel DI diesel engine, *SAE Technical Paper* 2009-01-0949. <https://doi.org/10.4271/2009-01-0949>
- EC. 2018. *Transport in the European Union: Current Trends and Issues*. European Commission (EC). 144 p. Available from Internet: <https://ec.europa.eu/transport/sites/transport/files/2018-transport-in-the-eu-current-trends-and-issues.pdf>
- EN 590:2013+A1:2017. *Automotive Fuels. Diesel. Requirements and Test Methods*.
- García Valladolid, P.; Tunestål, P.; Monsalve-Serrano, J.; García, A.; Hyvönen, J. 2017. Impact of diesel pilot distribution on the ignition process of a dual fuel medium speed marine engine, *Energy Conversion and Management* 149: 192–205. <https://doi.org/10.1016/j.enconman.2017.07.023>
- Heider, G. 1996. *Rechenmodell zur Vorausrechnung der NO-Emission von Dieselmotoren*. Dissertation. Technische Universität München, Deutschland. 144 S. (in German).
- Heider, G.; Woschni, G.; Zeilinger, K. 1998. 2-Zonen Rechenmodell zur Vorausrechnung der NO-Emission von Dieselmotoren, *MTZ – Motortechnische Zeitschrift* 59(11): 770–775. <https://doi.org/10.1007/BF03226479> (in German).
- HoC. 2012. *Sulphur Emissions by Ships*. Sixteenth Report of Session 2010–12. Volume II. Additional Written Evidence. House of Commons (HoC), Transport Committee, London, UK. 35 p. Available from Internet: <https://publications.parliament.uk/pa/cm201012/cmselect/cmtran/1561/1561vw.pdf>
- Hosmath, R. S.; Banapurmath, N. R.; Khandal, S. V.; Gaitonde, V. N.; Basavarajappa, Y. H.; Yaliwal, V. S. 2016. Effect of compression ratio, CNG flow rate and injection timing on the performance of dual fuel engine operated on honge oil methyl ester (HOME) and compressed natural gas (CNG), *Renewable Energy* 93: 579–590. <https://doi.org/10.1016/j.renene.2016.03.010>
- IMO. 2019a. *Greenhouse Gas Emissions*. International Maritime Organization (IMO). Available from Internet: <http://www.imo.org/en/OurWork/Environment/PollutionPrevention/AirPollution/Pages/GHG-Emissions.aspx>
- IMO. 2019b. *Prevention of Air Pollution from Ships*. International Maritime Organization (IMO). Available from Internet: <http://www.imo.org/en/OurWork/Environment/PollutionPrevention/AirPollution/Pages/Air-Pollution.aspx>
- IMO. 2016. *Studies on the Feasibility and Use of LNG as a Fuel for Shipping*. International Maritime Organization (IMO). 290 p. Available from Internet: <http://www.imo.org/en/OurWork/Environment/PollutionPrevention/AirPollution/Documents/LNG%20Study.pdf>
- ISO 6976:2016. *Natural Gas – Calculation of Calorific Values, Density, Relative Density and Wobbe Indices from Composition*.

- Ivanchenko, N. N.; Krasovskij, O. G.; Sokolov, S. S. 1983. *Vysokij nadduv dizelej*. Leningrad: Mashinostroenie. 198 s. (in Russian).
- Janbozorgi, M.; Ugarte, S.; Metghalchi, H.; Keck, J. C. 2009. Combustion modeling of mono-carbon fuels using the rate-controlled constrained-equilibrium method, *Combustion and Flame* 156(10): 1871–1885. <https://doi.org/10.1016/j.combustflame.2009.05.013>
- Kakaee, A.-H.; Rahnama, P.; Paykani, A. 2015. Influence of fuel composition on combustion and emissions characteristics of natural gas/diesel RCCI engine, *Journal of Natural Gas Science and Engineering* 25: 58–65. <https://doi.org/10.1016/j.jngse.2015.04.020>
- Kavtaradze, R. Z. 2008. *Teorija porshnevnyh dvigatelej: Special'nye glavy*. Moskva: MGTU im. N. Je. Baumana. 720 s. (in Russian).
- Lebedev, S. V.; Lebedeva, G. V.; Matievskij, D. D.; Reshetov V. I. 2003. *Formirovanie konstruktivnogo rjada porshnej dlja tipazha vysokooborotnyh forsirovannyh dizelej*. Altajskij gosudarstvennyj tehničeskij universitet im. I. I. Polzunova, Barnaul, Rossija. 89 s. (in Russian).
- Lebedevas, S.; Pukalskas, S.; Daukšys, V.; Rimkus, A.; Melaika, M.; Jonika, L. 2019. Research on fuel efficiency and emissions of converted diesel engine with conventional fuel injection system for operation on natural gas, *Energies* 12(12): 2413. <https://doi.org/10.3390/en12122413>
- Li, W.; Liu, Z.; Wang, Z. 2016. Experimental and theoretical analysis of the combustion process at low loads of a diesel natural gas dual-fuel engine, *Energy* 94: 728–741. <https://doi.org/10.1016/j.energy.2015.11.052>
- Liu, J.; Zhang, X.; Wang, T.; Zhang, J.; Wang, H. 2015. Experimental and numerical study of the pollution formation in a diesel/CNG dual fuel engine, *Fuel* 159: 418–429. <https://doi.org/10.1016/j.fuel.2015.07.003>
- Maghboul, A.; Saray, R. K.; Shafee, S.; Ghafouri, J. 2013. Numerical study of combustion and emission characteristics of dual-fuel engines using 3D-CFD models coupled with chemical kinetics, *Fuel* 106: 98–105. <https://doi.org/10.1016/j.fuel.2012.10.055>
- Maurya, R. K.; Mishra, P. 2017. Parametric investigation on combustion and emissions characteristics of a dual fuel (natural gas port injection and diesel pilot injection) engine using 0-D SRM and 3D CFD approach, *Fuel* 210: 900–913. <https://doi.org/10.1016/j.fuel.2017.09.021>
- Merker, G.; Schwarz, C.; Stiesch, G.; Otto, F. 2006. *Simulating Combustion: Simulation of Combustion and Pollutant Formation for Engine-Development*. Springer. 402 p. <https://doi.org/10.1007/3-540-30626-9>
- Mustafi, N. N.; Raine, R. R.; Verhelst, S. 2013. Combustion and emissions characteristics of a dual fuel engine operated on alternative gaseous fuels, *Fuel* 109: 669–678. <https://doi.org/10.1016/j.fuel.2013.03.007>
- Nithyanandan, K.; Lin, Y.; Donahue, R.; Meng, X.; Zhang, J.; Lee, C.-F. F. 2016. Characterization of soot from diesel-CNG dual-fuel combustion in a CI engine, *Fuel* 184: 145–152. <https://doi.org/10.1016/j.fuel.2016.06.028>
- Papagiannakis, R. G.; Rakopoulos, C. D.; Hountalas, D. T.; Rakopoulos, D. C. 2010. Emission characteristics of high speed, dual fuel, compression ignition engine operating in a wide range of natural gas/diesel fuel proportions, *Fuel* 89(7): 1397–1406. <https://doi.org/10.1016/j.fuel.2009.11.001>
- Rapolis, P.; Lebedeva, G.; Gudaitytė, I. 2013. Comparative analysis of diesel engine mathematical modelling packages for practical use on transport diesel engine operating on bio-diesel, in *Transbaltica 2013: the 8th International Conference: Selected Papers*, 9–10 May 2013, Vilnius, Lithuania, 173–178. <https://doi.org/10.3846/transbaltica2013.038>
- Rimkus, A.; Berioza, M.; Melaika, M.; Juknelevičius, R.; Bogdanovičius, Z. 2016. Improvement of the compression-ignition engine indicators using dual fuel (diesel and liquefied petroleum gas), *Procedia Engineering* 134: 30–39. <https://doi.org/10.1016/j.proeng.2016.01.035>
- Rimkus, A.; Melaika, M.; Matijošius, J. 2017. Efficient and ecological indicators of CI engine fuelled with different diesel and LPG mixtures, *Procedia Engineering* 187: 504–512. <https://doi.org/10.1016/j.proeng.2017.04.407>
- Thomson, H.; Corbett, J. J.; Winebrake, J. J. 2015. Natural gas as a marine fuel, *Energy Policy* 87: 153–167. <https://doi.org/10.1016/j.enpol.2015.08.027>
- Wang, T.; Zhang, X.; Zhang, J.; Hou, X. 2017. Numerical analysis of the influence of the fuel injection timing and ignition position in a direct-injection natural gas engine, *Energy Conversion and Management* 149: 748–759. <https://doi.org/10.1016/j.enconman.2017.03.004>
- Yousefi, A.; Birouk, M.; Guo, H. 2017. An experimental and numerical study of the effect of diesel injection timing on natural gas/diesel dual-fuel combustion at low load, *Fuel* 203: 642–657. <https://doi.org/10.1016/j.fuel.2017.05.009>
- Yousefi, A.; Birouk, M.; Lawler, B.; Gharehghani, A. 2015. Performance and emissions of a dual-fuel pilot diesel ignition engine operating on various premixed fuels, *Energy Conversion and Management* 106: 322–336. <https://doi.org/10.1016/j.enconman.2015.09.056>
- Zhang, C.; Zhou, A.; Shen, Y.; Li, Y.; Shi, Q. 2017. Effects of combustion duration characteristic on the brake thermal efficiency and NO_x emission of a turbo diesel engine fueled with diesel-LNG dual-fuel, *Applied Thermal Engineering* 127: 312–318. <https://doi.org/10.1016/j.applthermaleng.2017.08.034>